

Prenylated Flavonoids from the Roots of *Tephrosia rhodesica*

Yoseph Atilaw, Lois Muiva-Mutisya, Jonathan Bogaerts, Sandra Duffy, Arto Valkonen, Matthias Heydenreich, Vicky M. Avery, Kari Rissanen, Máté Erdélyi,* and Abiy Yenesew*

Cite This: *J. Nat. Prod.* 2020, 83, 2390–2398

Read Online

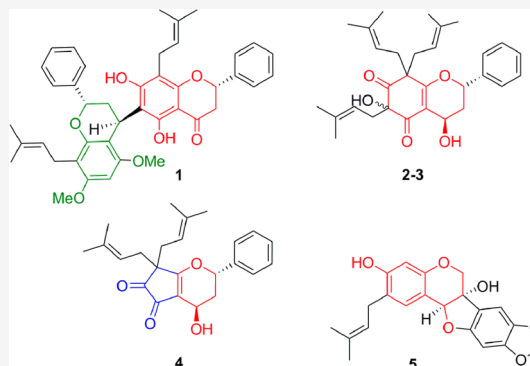
ACCESS |

Metrics & More

Article Recommendations

Supporting Information

ABSTRACT: Five new compounds—rhodimer (1), rhodiflavan A (2), rhodiflavan B (3), rhodiflavan C (4), and rhodacarpin (5)—along with 16 known secondary metabolites, were isolated from the CH_2Cl_2 – CH_3OH (1:1) extract of the roots of *Tephrosia rhodesica*. They were identified by NMR spectroscopic, mass spectrometric, X-ray crystallographic, and ECD spectroscopic analyses. The crude extract and the isolated compounds 2–5, 9, 15, and 21 showed activity (100% at 10 μg and IC_{50} = 5–15 μM) against the chloroquine-sensitive (3D7) strain of *Plasmodium falciparum*.



Tephrosia (Leguminosae) is a tropical and subtropical genus consisting of more than 400 species, 30 of which are native to Kenya.¹ These have provided a variety of new flavonoids, including flavanones, flavones, chalcones, pterocarpanes, and rotenoids, most of them prenylated and showing promising antiplasmodial, antifeedant, antileishmanial, estrogenic, anti-tumor, and antimicrobial activities.^{2–6} As part of our ongoing work on the genus *Tephrosia*,^{6,7} we now report the first phytochemical investigation of the roots of *Tephrosia rhodesica*, which showed antiplasmodial activity. The investigation of the root extract led to the isolation of five new compounds (1–5) and 16 known compounds (6–21). Herein, we describe their isolation, characterization, and activity against the chloroquine-sensitive (3D7) strain of *Plasmodium falciparum*.

RESULTS AND DISCUSSION

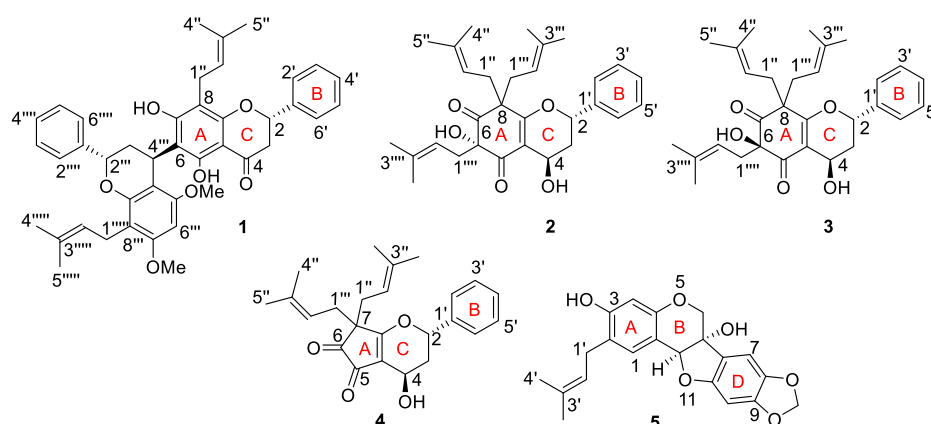
Applying silica gel gravity column chromatography, followed by Sephadex LH-20 gel filtration and preparative reverse-phase HPLC, 21 secondary metabolites were isolated from the roots of *T. rhodesica*. The structures of the isolated secondary metabolites were determined by NMR spectroscopic, mass spectrometric, and single-crystal X-ray diffractometric analyses. In addition to the five new secondary metabolites (1–5), the known tephrowatsin B (6),⁸ tephronine (7),⁹ glabranin (8),¹⁰ quercetol B (9),¹¹ maackiain (10),¹² 6a-hydroxymaackiain (11),¹³ pisatin (12),¹⁴ tephrosin (13),¹⁵ rotenone (14),¹⁶ 6-hydroxyrotenone (15),¹⁶ 12a-hydroxyrotenone (16),¹⁷ hildecarpin (17),¹⁸ 3-hydroxy-2-methoxy-8,9-methylenedioxypterocarpene (18),¹⁹ isoliquiritigenin (19),²⁰ D-pinitol (20),²¹ and tephrowatsin A (21)⁸ were identified by comparison of their observed and reported spectroscopic data (see pages S22–S34 in the Supporting Information).

Compound 1 was isolated as white crystals from CH_2Cl_2 – CH_3OH (1:1) solution. Its molecular formula was deduced as $\text{C}_{42}\text{H}_{44}\text{O}_7$ based on HREIMS ($[\text{M}]^+$ m/z 660.3095, calcd 660.3087) and NMR data analyses (see Table 1, as well as Figures S1–S6 in the Supporting Information). The ^1H NMR signals at δ_{H} 5.43 (H-2), 5.06 (H-2'''), 2.84 and 3.07 (H-3a-b), 2.18 and 2.31 (H-3'''), and 4.66 (H-4'''), along with the ^{13}C NMR signals at δ_{C} 78.6 (C-2), 75.4 (C-2'''), 43.7 (C-3), 36.9 (C-3'''), 196.3 (C-4), and 26.8 (C-4''') were consistent with a flavanone-flavan dimer core structure^{22,23} that was corroborated by the UV absorptions of λ_{max} = 230, 290, and 350 nm. The NMR data (Table 1) indicated the presence of two sets of unsubstituted aromatic rings, two sets of prenyl groups, two hydroxy, and two methoxy groups. This is consistent with a 5-hydroxyflavanone moiety possessing an unsubstituted ring B, along with a ring A substituted with prenyl at C-8 (δ_{C} 108.1) and two hydroxy groups, δ_{H} 12.61 (HO-5) and 6.80 (HO-7) at C-5 (δ_{C} 159.3) and C-7 (δ_{C} 162.8). Accordingly, C-6 (δ_{C} 109.8) connects the flavanone to the flavan moiety. Whereas the placement of a hydroxy group at C-7 was based on biogenetic considerations,²⁴ and on the chemical shift of the HO-5 hydrogen (δ_{H} 12.61), suggesting its involvement in an intramolecular hydrogen bond; the placement of the prenyl group at C-8 (δ_{C} 108.1) rather than at C-6 (δ_{C} 109.8) was

Received: March 5, 2020

Published: August 13, 2020



Table 1. NMR Spectroscopic Data (800 MHz, CDCl₃) for Rhodimer (1)

position	$\delta_{\text{C, type}}$	δ_{H} (J, in Hz)	HMBC
2	78.6, CH	5.43, dd (2.9, 13.1)	C-4, C-1', C-2'/6', C-8a
3	43.7, CH ₂	2.84, dd (2.9, 17.1) 3.07, dd (13.1, 17.1)	C-2, C-4, C-1', C-4, C-4a, C-1'
4	196.3, C=O		
4a	100.4, C		
5	159.3, C=O		
6	109.8, C		
7	162.8, C=O		
8	108.1, C		
8a	157.6, C=O		
1'	139.1, C		
2'/6'	125.9, CH	7.47, m	C-2, C-2'/6', C-3'/5'
3'/5'	128.7, CH	7.43, m	C-1', C-3'/5'
4'	128.5, CH	7.39, m	C-2'/6'
1''	21.8, CH ₂	3.18, br t	C-7, C-8, C-8a, C-3'', C-2''
2''	122.5, CH	5.15, br t	C-1'', C-4'', C-5''
3''	131.6, C		
4''	17.8, CH ₃	1.57, s	C-3'', C-2'', C-5''
5''	25.8, CH ₃	1.65, s	C-3'', C-2'', C-4''
OH-5		12.61, s	C-5, C-6, C-4a, C-4, C-7
OH-7		6.80, s	C-6, C-8, C-8a, C-7, C-4a
2'''	75.4, CH	5.06, dd (2.0, 11.5)	C-4''', C-1''', C-2'''/6''', C-8a
3'''	36.9, CH ₂	2.18, dt (2.0, 6.0, 14.0) 2.31, dt (2.0, 11.5, 14.0)	C-1''', C-4''', C-6, C-4''', C-4'''a, C-6
4'''	26.8, CH	4.66, dd (2.0, 6.0)	C-2''', C-3''', C-4'''a, C-5''', C-8'''a, C-5, C-6, C-7
4'''a	102.8, C		
5'''	157.5, C=O		
6'''	88.4, CH	6.17, s	C-4''', C-4'''a, C-5''', C-7''', C-8''', C-1''''' (w)
7'''	158.6, C=O		
8'''	110.5, C		
8'''a	154.3, C=O		
1''''	141.4, C		
2''''/6''''	126.0, CH	7.38, m	C-2''', C-2''''/6''', C-3''''/5''''
3''''/5''''	128.3, CH	7.34, m	C-3''''/5''', C-1''''
4''''	127.6, CH	7.29, m	C-2''''/6''''
1'''''	21.9, CH ₂	3.35, br t	C-8''', C-8a''', C-7''', C-3''''', C-2'''''
2'''''	123.2, CH	5.24, br t	C-1''''', C-4''''', C-5'''''
3'''''	130.8, C		
4'''''	17.8, CH ₃	1.66, s	C-2''''', C-3''''', C-5'''''
5'''''	25.9, CH ₃	1.68, s	C-2''''', C-3''''', C-4'''''
OMe-5''''	55.9, C=O	3.73, s	C-5''''
OMe-7''''	55.8, C=O	3.87, s	C-7''''

based on the HMBC correlation of CH₂-1'' (δ_{H} 3.18) with C-7 (δ_{C} 162.8), C-8 (δ_{C} 108.1), C-8a (δ_{C} 157.6), C-3'' (δ_{C} 131.6), C-2'' (δ_{C} 122.5), and of H-2 (δ_{H} 5.43) with C-4 (δ_{C} 196.3), C-1' (δ_{C} 139.1), C-2'/C-6' (δ_{C} 125.9), C-8a (δ_{C}

157.6). The identity of the other half of the molecule was established as a 5,7-dimethoxy-8-prenylflavan moiety based on the NMR data (Table 1). Hence, its ¹H NMR spectrum revealed the presence of an unsubstituted aromatic ring (ring

E) [δ_{H} 7.38 (H-2''''/6'''), 7.34 (H-3''''/5'''), 7.29 (H-4''')], two methoxy groups at δ_{H} 3.73 (OMe-5''') and 3.87 (OMe-7''') and a prenyl side chain [δ_{H} 3.35 (H-1'''), 5.24 (H-2'''), 1.66 (H-4'''), and 1.68 (H-5''')], and a singlet at δ_{H} 6.17 (H-6'''). The placement of the two methoxy groups was established based on the HMBC correlation of H-6''' (δ_{H} 6.17) with C-4''' (δ_{C} 102.8), C-5''' (δ_{C} 157.5), and C-7''' (δ_{C} 158.6). The prenyl group was positioned at C-8''' (δ_{C} 110.5) based on the HMBC cross-peaks of H₂-1'''' (δ_{H} 3.35) to C-8''' (δ_{C} 110.5), C-8a''' (δ_{C} 154.3), and C-7''' (δ_{C} 158.6). Methoxy groups were placed at C-5''' (δ_{C} 157.5) and C-7''' (δ_{C} 158.6) upon biogenetic considerations,²⁴ as well as based on the HMBC correlations of MeO-5''' (δ_{H} 3.73) to C-5''' (δ_{C} 157.5), and of MeO-7''' (δ_{H} 3.87) to C-7''' (δ_{C} 158.6). This assignment was corroborated by the NOEs of MeO-5''' (δ_{H} 3.73) and MeO-7''' (δ_{H} 3.87) with H-6''' (δ_{H} 6.17). The C-6 (δ_{C} 109.8) to C-4''' (δ_{C} 26.8) linkage of the flavanone and the flavan moieties was confirmed by the HMBC correlations of H-4''' (δ_{H} 4.66) with C-5 (δ_{C} 159.3), C-6 (δ_{C} 109.8), and C-7 (δ_{C} 162.8), and of H₂-3''' (δ_{H} 2.18 and 2.31) with C-6 (δ_{C} 109.8). Because of its three stereocenters at C-2, C-2''', and C-4''', **1** has eight possible stereoisomers. The large $^3J_{2,3} = 13.1$ Hz indicated H-2 to be axial, and thereby ring B to be equatorial. Based on the available literature on the flavanones of this genus, C-2 is expected to be *S*-configured.^{1,25} Similarly, the large $^3J_{2''',3'''} = 11.5$ Hz suggests H-2''' to be axial, and accordingly ring B of the flavan moiety to be equatorially oriented. Furthermore, based on the literature,²⁵ C-2''' is also expected to be *S*-configured as in the flavanones and flavans of this genus. The $^3J_{3a''',4'''} = 2.0$ suggests the axial–equatorial or equatorial–equatorial orientation of the involved protons, whereas $^3J_{3b''',4'''} = 6.0$ Hz gauche orientation, suggesting H-4''' to be axially oriented and, consequently, the flavan moiety to occupy the more favorable equatorial orientation with C-4''' being *R*-configured.²⁵ The NOE correlation of H-2''' (δ_{H} 5.06) and HO-7 (δ_{H} 6.80) reveals the flavanone and H-2''' to be oriented in the same direction. This absolute configuration (2*S*,2'''*S*,4'''*R*), proposed on the basis of biogenetic considerations and NMR analyses was subsequently confirmed by single-crystal X-ray crystallography (Figure 1). Thus, based on the above spectroscopic data, this new compound, rhodimer (**1**), was characterized as (2*S*,2'''*S*,4'''*R*)-5,7-dihydroxy-5''',7'''-dimethoxy-8,8'''-bis(3-methylbut-2-en-1-yl)-2',2'''-diphenyl-[4''',6-bichroman]-4-one.

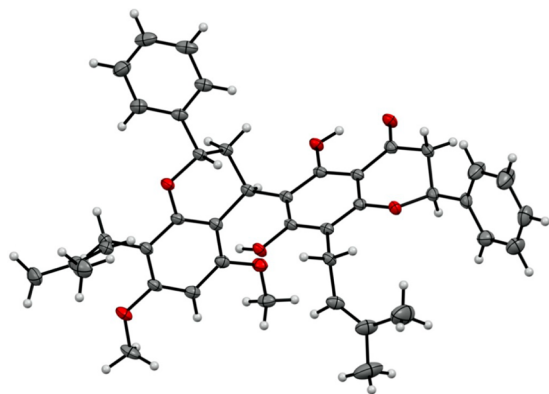


Figure 1. Single crystal X-ray structure of compound **1** with the thermal displacement parameters at 40% probability level.

Compound **2** was isolated as an oily paste and was assigned the molecular formula $\text{C}_{30}\text{H}_{38}\text{O}_5$, based on HRESIMS ($[\text{M} + \text{H}]^+$ m/z 479.2493, calcd 479.2753) and NMR data analyses (see Table 2, as well as Figures S9–S14 in the Supporting Information). The ^1H NMR signals at δ_{H} 5.22 (H-2), 1.80 (H-3_{ax}), 2.31 (H-3_{eq}), and 4.99 (H-4), along with the ^{13}C NMR signals at δ_{C} 76.1 (C-2), 37.0 (C-3), and 57.4 (C-4), suggested it to be a flavan-4-ol derivative, which was corroborated by the UV absorptions $\lambda_{\text{max}} = 240$ and 290 nm. The characteristic flavan-4-ol ring C of **2** was confirmed by the HMBC correlations of H-4 (δ_{H} 4.99) with C-2 (δ_{C} 76.1), C-3 (δ_{C} 37.0), C-5 (δ_{C} 194.7), C-4a (δ_{C} 114.9), and C-8a (δ_{C} 171.0), and by the COSY correlations of H-2 (δ_{H} 5.22) with CH₂–3 (δ_{H} 2.31 and 1.80), and of the latter with H-4 (δ_{H} 4.99). The six methyl (H₃-4'', H₃-4''', H₃-4''', H₃-5'', H₃-5''', and H₃-5'''), along with the three methine signals (H-2'', H-2''', and H-2'''), were diagnostic for three prenyl groups. The NMR signals of H-2'/6', H-3'/5', and H-4' (Table 2) further suggested ring B to be unsubstituted and, hence, all three prenyl groups to be connected to ring A. This ring is oxygenated at C-5 (δ_{C} 194.7) and C-7 (δ_{C} 206.4), with their placement having been derived from biogenetic considerations.²⁴ An additional oxygenation is presented at C-6 (δ_{C} 83.3), which uncharacteristically is an sp^3 hybridized carbon. Prenyl substitution at this carbon was confirmed by the HMBC correlation of H-2'''' (δ_{H} 4.99) with C-6 (δ_{C} 83.3). The location of the other two prenyl groups at C-8 (δ_{C} 58.3), also sp^3 hybridized, was established from the ^3J HMBC correlations of H-2'' (δ_{H} 5.03, *m*) and H-2''' (δ_{H} 4.66, *m*) with C-8 (δ_{C} 58.3). Moreover, CH₂–1'' (δ_{H} 2.60 and 2.81) and CH₂–1''' (δ_{H} 2.46 and 2.77) showed HMBC cross-peaks with C-7 (δ_{C} 206.4) and C-8a (δ_{C} 171.0), whereas CH₂–1'''' (δ_{H} 2.71 and 2.25) with C-5 (δ_{C} 194.7), confirming that ring A is fully substituted. Based on the above data, compound **2** was characterized as 4,6-dihydroxy-6,8,8-tris(3-methylbut-2-en-1-yl)-2-phenyl-2,3,4,8-tetrahydro-5*H*-chromene-5,7(6*H*)-dione. Its configurational assignment is discussed below, together with that of the structurally closely related compound **3**.

Compound **3** was isolated as an oily paste and was assigned the molecular formula $\text{C}_{30}\text{H}_{38}\text{O}_5$ based on HRESIMS ($[\text{M} + \text{H}]^+$ m/z 479.2493, calcd 479.2753) and NMR data (see Table 2, as well as Figures S16–S21 in the Supporting Information). The ^1H NMR signals at δ_{H} 5.24 (H-2), 2.00 and 2.30 (CH₂–3), and δ_{H} 4.55 (H-4) and ^{13}C NMR signals at δ_{C} 76.2 (C-2), 36.5 (C-3), and 59.5 (C-4) suggested **3** to be a flavan derivative with identical core structure, 4,6-dihydroxy-6,8,8-tris(3-methylbut-2-en-1-yl)-2-phenyl-2,3,4,8-tetrahydro-5*H*-chromene-5,7(6*H*)-dione to compound **2**. The highly similar NMR data of **2** and **3** (Table 2) indicated these compounds to be stereoisomers.

Compounds **2** ($[\alpha]_{\text{D}} +66.1$) and **3** ($[\alpha]_{\text{D}} +17.5$) are both dextrorotatory (for details, see the Experimental Section) and, hence, are diastereomers (as enantiomers would be expected to rotate plan-polarized light in opposite directions). The large coupling constant $^3J_{2,3\text{ax}}$ (12.6 Hz in both **2** and **3**) is consistent with H-2 being axial and ring B of both compounds to occupy the more favorable equatorial orientation.²⁵ The $^3J_{3\text{ax},4}$ (4.2 Hz for **2**, and 3.7 Hz for **3**) and $^3J_{3\text{eq},4}$ (1.9 Hz in **2**, 2.3 Hz in **3**) are small, suggesting H-4 to be equatorial and hence HO-4 to be axial in both compounds, according to Pouget et al.²⁶ This is further corroborated by the 3.4 Å H-2–H-4 interatomic distance of **3**, estimated based on the NOE cross-peak intensities using H-3a/b as an internal reference (1.8 Å; see

Table 2. NMR Spectroscopic Data (800 MHz, CDCl₃) for Rhodiflavan A (2) and Rhodiflavan B (3)

position	2			3		
	δ_C , type	δ_H , m (J in Hz)	HMBC	δ_C , type	δ_H , m (J in Hz)	HMBC
2	76.1, CH	5.22, dd (12.6, 2.3)	C-3, C-4, C-1', C-2', C-6'	76.2, CH	5.24, dd (12.6, 2.3)	C-3, C-4, C-1', C-2', C-6'
3	37.0, CH ₂	2.31, ddd (14.6, 2.3, 1.9)	C-4, C-4a	36.5, CH ₂	2.30, dt (14.6, 2.3, 2.0)	C-4, C-4a
		1.80, ddd (14.6, 12.6, 4.2)	C-1', C-2		2.00, ddd (14.6, 12.6, 3.6)	C-2, C-1'
4	57.4, CH	4.99, m	C-2, C-3, C-5, C-4a, C-8a	59.5, CH	4.55, dd (2.0, 3.6)	C-2, C-4a, C-8a, C-5
4a	114.9, C			114.2, C		
5	194.7, C=O			197.0, C=O		
6	83.3, C-OH			83.4, C-OH		
7	206.4, C=O			207.2, C=O		
8	58.3, C			58.3, C		
8a	171.0, C-O			171.0, C-O		
1'	138.9, C			139.2, C		
2', 6'	125.9, CH	7.40, m	C-2, C-2', C-4', C-6'	125.9, CH	7.40, m	C-2, C-4', C-2', C-6'
3', 5'	128.7, CH	7.43, m	C-1', C-3', C-5'	128.7, CH	7.43, m	C-1', C-3', C-5'
4'	128.5, CH	7.39, m	C-1', C-2', C-6'	128.5, CH	7.39, m	C-1', C-2', C-6'
1''	35.0, CH ₂	2.81, dd (14.2, 9.2)	C-7, C-8, C-8a, C-2'', C-3'', C-1'''	34.5, CH ₂	2.89, dd (14.2, 9.8)	C-7, C-8, C-8a, C-2'', C-3'', C-1'''
		2.60, dd (6.3, 14.2)	C-7, C-8, C-8a, C-2'', C-3'', C-1'''		2.59, m	C-7, C-8, C-8a, C-2'', C-3'', C-1'''
1'''	38.5, CH ₂	2.77, m	C-7, C-8, C-8a, C-2''', C-3''', C-1''	38.5, CH ₂	2.69, dd (13.5, 7.3)	C-7, C-8, C-8a, C-2''', C-3''', C-1''
		2.46, dd (13.7, 8.2)	C-7, C-8, C-8a, C-2''', C-3''', C-1''		2.43, dd (13.5, 8.7)	C-7, C-8, C-8a, C-2''', C-3''', C-1''
1''''	38.5, CH ₂	2.71, dd (14.9, 6.3)	C-6, C-5, C-2''''	38.2, CH ₂	2.63, dd (14.7, 8.7)	C-6, C-5, C-2''''
		2.25, dd (15.0, 5.7)	C-6, C-5, C-2''''		2.18, m	C-6, C-5, C-2''''
2''	118.8, CH	5.03, m	C-1'', C-4'', C-5''	118.8, CH	5.13, m	C-8, C-1'', C-4'', C-5''
2'''	117.4, CH	4.66, m	C-8, C-1''', C-4''', C-5'''	117.4, CH	4.71, m	C-8, C-1''', C-4''', C-5'''
2''''	115.6, CH	4.99, m	C-6, C-4''', C-5''''	115.5, CH	4.97, m	C-6, C-4''', C-5''''
3''	136.0, C			136.0, C		
3'''	136.9, C			136.9, C		
3''''	136.9, C			136.9, C		
4''	26.0, CH ₃	1.64, s	C-1'', C-2'', C-5''	18.0, CH ₃	1.61, s	C-1'', C-2'', C-5''
4'''	18.1, CH ₃	1.52, s	C-1''', C-2''', C-5'''	17.8, CH ₃	1.52, s	C-1''', C-2''', C-5'''
4''''	26.0, CH ₃	1.71, s	C-2''', C-3''', C-5''''	25.9, CH ₃	1.71, s	C-2''', C-3''', C-5''''
5''	18.1, CH ₃	1.59, s	C-1'', C-2'', C-4''	26.0, CH ₃	1.68, s	C-1'', C-2'', C-4''
5'''	25.8, CH ₃	1.55, s	C-1'', C-2'', C-4''	25.7, CH ₃	1.56, s	C-1'', C-2'', C-4''
5''''	17.9, CH ₃	1.55, s	C-2''', C-3''', C-4''''	17.9, CH ₃	1.54, s	C-2''', C-3''', C-4''''

Figure S23 in the Supporting Information). This distance was computed to 2.3 Å for the (2*S**,4*S**) diastereomer, and 3.7 Å for the (2*S**,4*R**) configured C-ring, using Boltzmann averaging of the H-2–H-3 distances of the output conformers of Monte Carlo conformational searches (see [Experimental Section](#) for details; this distance was not measured for **2**, because of signal overlap). Based on biogenetic considerations discussed for compound **1** and the NMR data, compounds **2** and **3** are C-6 epimers and possess a (2*S*,4*R*) absolute configuration. In order to determine their absolute configuration, their electronic circular dichroism (ECD) spectra (Figure 2) were recorded. The observed Cotton effects supported the ORD-based suggestion of the diastereomeric relationship of **2** and **3** as enantiomers are expected to show mirror-image ECD spectra. The comparison of the experimental spectra with those reported for flavan-4-ols¹¹ did not allow configurational assignment, because of the dissimilarity of rings A of **2** and **3**, compared to those of the reported compounds. Consequently, the Boltzmann-weighted ECD spectra of the possible diastereomers were calculated using

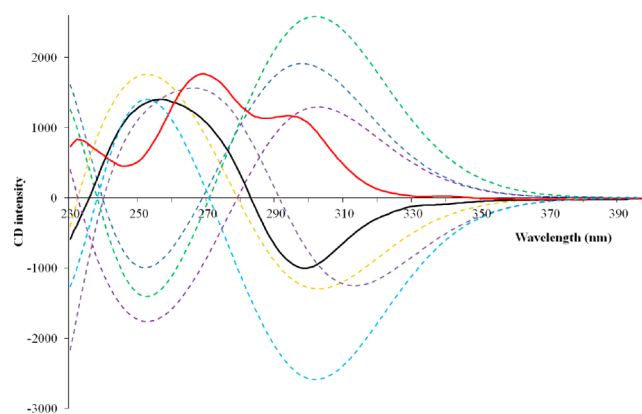


Figure 2. ECD spectra of compounds **2** (black) and **3** (red) along with the calculated spectra of the stereoisomers [(2*S*,4*R*,6*S*) yellow, (2*S*,4*R*,6*R*) blue, (2*S*,4*S*,6*R*) green, (2*S*,4*S*,6*S*) lilac, (2*R*,4*S*,6*R*) pink, (2*R*,4*S*,6*S*) light blue]. See details of the ECD calculations in the [Experimental Section](#).

Table 3. ^1H and ^{13}C NMR Spectroscopic Data (800 MHz, CDCl_3) for Rhodiflavan C (4)

position	δ_{C} , type	δ_{H} , m (J in Hz)	HMBC
2	78.8, CH	5.45, dd (12.3, 2.2)	C-3, C-4, C-1', C-2'/C-6'
3	37.0, CH_2	2.31, dt (14.8, 2.3) 2.02, ddd (14.9, 12.3, 3.5)	C-4, C-4a C-2, C-1'
4	55.6, CH	4.86, m	C-2, C-5, C-4a, C-7a
4a	125.9, C		
5	184.5, $\text{C}=\text{O}$		
6	203.4 $\text{C}=\text{O}$		
7	52.9, C,		
7a	188.6, C–O		
1'	137.9, C		
2', 6'	126.3, CH	7.40, m	C-2, C-2', C-4', C-6'
3', 5'	128.9, CH	7.46, m	C-1', C-2', C-3', C-5', C-6'
4'	129.1, CH	7.43, m	C-2', C-6', C-3', C-5'
1''	32.8, CH_2	2.51, dd (14.3, 7.2) 2.42, dd (14.3, 7.9)	C-5, C-6, C-7, C-7a, C-2'', C-3'', C-1''' C-5, C-6, C-7, C-7a, C-2'', C-3'', C-1'''
1'''	32.6, CH_2	2.56, dd (14.2, 7.2) 2.44, dd (14.2, 7.9)	C-5, C-6, C-7, C-7a, C-2''', C-3''', C-1'' C-5, C-6, C-7, C-7a, C-1'', C-2''', C-3'''
2''	116.9, CH	4.86, m	C-8, C-1'', C-4'', C-5''
2'''	116.9, CH	4.86, m	C-8, C-1''', C-4''', C-5'''
3''	136.6, C		
3'''	136.8, C		
4''	25.9, CH_3	1.61, s	C-1'', C-2'', C-5''
4'''	25.9, CH_3	1.61, s	C-1''', C-2''', C-4'''
5''	17.9, CH_3	1.57, s	C-1'', C-2'', C-5''
5'''	17.8, CH_3	1.56, s	C-1''', C-2''', C-4'''

Table 4. ^1H and ^{13}C NMR Spectroscopic Data (800 MHz, CDCl_3) of Compound 5

position	δ_{C} , type	δ_{H} , m (J in Hz)	HMBC
1	131.8, CH	7.20, s	C-3, C-11a, C-4a, C-1'
2	121.8, C		
3	155.8, C–O		
4	104.0, CH	6.40	C-2, C-3, C-11b, C-4a
4a	154.1, C–O		
6	69.6, CH_2	3.95, d (11.5) 4.15, d (11.5)	C-4a, C-6b, C-11a C-4a, C-6a, C-6b, C-11a
6a	77.2, C–H		
6b	119.0, C		
7	103.0, CH	6.80, s	C-6a, C-8, C-9, C-10a
8	142.4, C–O		
9	149.7, C–O		
10	94.2, CH	6.81, s	C-8, C-9, C-6b, C-10a
10a	149.7, C		
11a	84.8, C–H	5.25, s	C-1, C-4a, C-6, C-6a, C-11b, C-10a
11b	112.1, C		
$\text{OCH}_2\text{O-8, 9}$	101.5, CH_2	5.91, d (1.4) 5.94, d (1.4)	C-8, C-9
1'	29.2, CH_2	3.32, d (7.2)	C-1, C-3, C-2', C-3'
2'	121.8, CH	5.31, m	C-4', C-5', C-1'
3'	135.8, C		
4'	17.9, CH_3	1.78, s	C-2', C-3', C-5'
5'	25.8, CH_3	1.78, s	C-2', C-3', C-4'

the TD-DFT method (see [Experimental Section](#) for details), and compared to those obtained experimentally for **2** and **3** ([Figure 2](#)). The experimental ECD spectrum of **2** showed a negative Cotton effect at ca. 300 nm, positive at 260, and negative at 230 nm, best matched with the calculated spectrum of the (2*S*,4*R*,6*S*) isomer. Nonetheless, the mirror imaged spectrum of the (2*S*,4*R*,6*R*) isomer, corresponding to a (2*R*,4*S*,6*S*) configuration, shows similar Cotton effects. Furthermore, the calculated spectra of the (2*S*,4*R*,6*S*) and

(2*S*,4*S*,6*S*) isomers are remarkably similar, and the same goes for the other two calculated isomers. None of these show agreement with the experimentally obtained ECD spectrum of **3**. Based on the above spectroscopic evidence, the new compounds rhodiflavan A (**2**) and B (**3**) are characterized as diastereomers of 4,6-dihydroxy-6,8,8-tris(3-methylbut-2-en-1-yl)-2-phenyl-2,3,4,8-tetrahydro-5*H*-chromene-5,7(6*H*)-dione, with (2*S**,4*R**,6*S**) and (2*S**,4*R**,6*R**) relative configurations, respectively.

Compound **4** was isolated as an oily paste. Its molecular formula was deduced as $C_{24}H_{28}O_4$ based on HREIMS (m/z $[M]^+$ 381.2062, calcd 381.2066) and NMR data (see Table 3, as well as Figures S23–S28 in the Supporting Information) analyses. The 1H NMR signals at δ_H 5.45 (H-2), 2.02 (H-3_{ax}), 2.31 (H-3_{eq}), and 4.86 (H-4), the ^{13}C NMR signals at δ_C 78.8 (C-2), 37.0 (C-3), and 55.6 (C-4), along with the UV λ_{max} at 230 and 270 nm suggested compound **4** to have an analogous ring C to those of **2** and **3**. Its 1H NMR signals at δ_H 7.4 (H-2'/6'), 7.46 (H-3'/5'), and 7.43 (H-4') indicated ring B to be unsubstituted. The lack of aromatic protons for ring A suggested it to be fully substituted. As rings B and C were fully assigned, the carbonyl groups at δ_C 184.5 (C-5) and 203.4 (C-6), and the two prenyl groups (see Table 3 for signals 1''–5'', and 1'''–5''') could only be related to ring A. The HMBC correlations of H-2'' (δ_H 4.86) and H-2''' (δ_H 4.86) with C-7 (δ_C 52.9) revealed the two prenyl groups to be both attached to C-7. Both methylene groups CH_2 –2'' (δ_H 4.86) and CH_2 –2''' (δ_H 4.86) showed HMBC correlation to δ_C 188.6 (C-7a), δ_C 203.4 (C-6), and δ_C 52.9 (C-7), indicating the placement of the two carbonyl groups at C-5 and C-6, which, being a five-membered ring, is unique for the genus *Tephrosia*. The difference in the chemical shifts of C-5 (δ_C 184.5) and C-6 (δ_C 203.4) is rationalized by the strong intramolecular hydrogen bond of HO-4 and the oxygen of the C-5 carbonyl group, and C-5 has strong conjugation with C-7a through the 4a (7a) double bond. The observed mass and NMR data (vide supra), the UV spectrum only showing a benzenoid band, and the HMBC of H-4 (δ_H 4.86) with C-5 (δ_C 184.5) corroborate the proposed structure. It is optically active ($[\alpha]_D^{+90}$ (c 0.001, CH_2Cl_2), and its ECD spectrum (see Figure S30 in the Supporting Information) shows a positive Cotton effect at λ 300–340 nm and a negative one at 275 nm. Based on the similarity of the NMR data (δ , J , Table 3) of H-2, H-3, and H-4 (ring C) of **4** to those of compounds **2** and **3** (Table 2), compound **4** was assigned the (2*S**,4*R**) relative configuration. Therefore, based on the above spectroscopic data, this unique compound, rhodiflavan C (**4**), was characterized as (2*S**,4*R**)-4-hydroxy-7,7-bis(3-methylbut-2-en-1-yl)-2-phenyl-2,3,4,7-tetrahydrocyclopenta[b]pyran-5,6-dione.

Compound **5** was isolated as an amorphous solid and was assigned the molecular formula $C_{21}H_{20}O_6$ based on HRESIMS ($[M + H]^+$ m/z obs 369.1367) and NMR data (see Table 4, as well as Figures S31–S36 in the Supporting Information) analyses. It showed characteristic UV (λ_{max} 230, 190, 310, and 350 nm), 1H NMR [δ_H 3.95 and 4.15 (CH_2 –6), 5.25 (H-11a)], and ^{13}C NMR data [δ_C 69.6 (C-6), 77.2 (C-6a), 84.8 (C-11a)] for a 6a-hydroxypterocarpan skeleton. The NMR data further indicated the presence of a prenyl group [δ_H 3.32 (H-1'), 5.31 (H-2'), 1.78 (H-3'-4' and H-3'-5'), and δ_C 29.2 (C-1') 121.8 (C-2'), 135.8 (C-3'), 17.9 (C-4'), 25.8 (C-5')] connected to C-2, as revealed by HMBC cross-peaks of H-1' (δ_H 7.20) with C-1' (δ_C 29.2), and of CH_2 –1' (δ_H 3.32) with C-1 (δ_C 131.8) and C-3 (δ_C 155.8). The position of the prenyl group was confirmed by the NOE correlation between H-1 (δ_H 7.20) and CH_2 –1' (δ_H 3.32). Hence, ring A is substituted with a prenyl group at C-2 and a hydroxy group at C-3. Its C-1 and C-4 are unsubstituted as evidenced by the two singlets in its 1H NMR data. In ring D, the NMR data (Table 4) indicated the presence of an 8,9-methylenedioxy group (δ_H 5.91 and 5.94; δ_C 101.5) and two *p*-substituted aromatic protons at δ_H 6.80 (H-7) and δ_H 6.81 (H-10). The NMR spectra of this compound showed resemblance to those of previously

published pterocarpan.^{7,27–29} The absolute configuration at the B/C-ring junction was determined as (6*aS*,12*aS*), based on the ECD spectrum (see Figure S34 in the Supporting Information), which exhibited a positive and negative Cotton effect at 309 nm and 241 nm, respectively.³⁰ Based on the above spectroscopic data, this new compound, rhodacarpin (**5**), was characterized as (6*aS*,12*aS*)-2-(3-methylbut-2-en-1-yl)-6*H*-[1,3]dioxolo[4',5':5,6]benzofuro[3,2-*c*]chromene-3,6*a*-(12*aH*)-diol.

The crude extract of the roots of *T. rhodesica* and the isolated compounds were tested for antiparasitic activity using a previously established protocol.³¹ The crude extract gave 100% growth inhibition of the chloroquine-sensitive (3D7) strain of *Plasmodium falciparum* at 10 μ g/mL concentration, whereas the isolated compounds **2**, **3**, **4**, **5**, **9**, and **15** showed moderate activities (Table 5). Among the tested compounds, **3** showed the highest activity (IC_{50} = 5.7 ± 1.9 μ M).³²

Table 5. In Vitro Antiparasitic Activities (IC_{50}) of Isolated Compounds against 3D7 Strains of *P. falciparum*^a

sample	IC_{50} , μ M (Pf3D7)	LD_{50} (HEK-293)
<i>T. rhodesica</i> (roots) crude extract	100% active at 10 μ g/mL	
Rhodiflavan A (2)	7.3 ± 1.8	71% at 40 μ M
Rhodiflavan B (3)	5.7 ± 1.9	34% at 40 μ M
Rhodiflavan C (4)	7.0 ± 2.4	101% at 40 μ M
Rhodacarpin (5)	10.2 ± 0.2	27% at 40 μ M
Quercetol B (9)	7.4 ± 0.3	87% at 40 μ M
6-Hydroxyrotenone (15)	8.6 ± 2.6	10.9 μ M
Tephrowatsin A (21)	14.5 ± 0.7	
Chloroquine	0.0047	
Artesunate	0.00067	

^aCompounds were tested independently either two or three times against Pf3D7. All compounds were tested in a single experiment against HEK 293 mammalian cells (LD_{50}).

In conclusion, five new compounds—rhodimer (**1**), rhodiflavan A (**2**), rhodiflavan B (**3**), rhodiflavan C (**4**), and rhodacarpin (**5**)—were isolated from the roots of *Tephrosia rhodesica*, along with 16 known natural products. Rhodimer is an unusual flavanone-flavan dimer, whereas rhodiflavan C has a five-membered A-ring, which is unprecedented for this genus. The crude root extract and several of its isolated constituents showed activities against the chloroquine-sensitive (3D7) strain of *Plasmodium falciparum*.

EXPERIMENTAL SECTION

General Experimental Procedures. Optical rotations were measured on a PerkinElmer 341-LC system, whereas ECD experiments were performed on a Jasco Model J-715 spectropolarimeter. UV spectra were recorded on a Specord S600 (Analytik Jena AG) spectrophotometer. Melting points were obtained on a Büchi Melting Point B-545 Switzerland apparatus; NMR spectra were acquired on a Bruker Avance III HD 800 MHz NMR spectrometer equipped with a TCI cryogenic probe and were processed with the MestReNova 10.0 software, using the solvent residual signal ($CDCl_3$ δ_H 7.26; δ_C 77.16) as chemical shift reference. LC-ESIMS data were obtained on a Micromass GC-TOF micro mass spectrometer (Micromass, Wythenshawe, Waters, Inc., U.K.), using direct inlet, and 70 eV ionization voltage. TLC was performed on Merck precoated silica gel 60 F254 plates. Column chromatography was run on silica gel 60 (70–230 mesh). Gel filtration was done on Sephadex LH-20. Preparative HPLC was performed on a Waters 600E instrument using the

Chromulan (Pikron, Ltd.) software and an RP C₈ Kromasil (250 mm × 55 mm) column eluting with repeated CH₃OH–H₂O (5 to 95) gradients. Single-crystal X-ray data of **1** were collected at 120 K on an Agilent SuperNova dual wavelength diffractometer with a microfocus X-ray source and multilayer optics monochromatized Cu K α (λ = 1.54184 Å) radiation.

Plant Material. The roots of *Tephrosia rhodesica* were collected in April 2015 from Kilungu Hills in Makueni County, Kenya. The plant specimen was identified by Mr. Patrick C. Mutiso of the School of Biological Sciences, the University of Nairobi. A voucher specimen (Mutiso-842/April 2015) was deposited at the University Herbarium of the University of Nairobi, Kenya.

Extraction and Isolation. The air-dried roots (2 kg) of *T. rhodesica* were ground and extracted with CH₂Cl₂–CH₃OH (1:1) (3 × 2 L) by percolation at room temperature to yield 70 g of a dark brown paste after evaporation of the solvent. A portion of the extract (37 g) was subjected to column chromatography over silica gel (400 g) eluting with a mixture of *iso*-hexane containing increasing amounts of EtOAc. The fraction eluted with 1% EtOAc in *iso*-hexane was purified by preparative HPLC (CH₃OH–H₂O gradient elution) to give tephrowatsin B (**6**, 20 mg).⁸ The fraction eluted with 3% EtOAc in *iso*-hexane was purified by column chromatography on a Sephadex LH-20 column (CH₂Cl₂–CH₃OH; 1:1) to give tephirone (**7**, 200 mg)⁹ and glabranin (**8**, 100 mg).¹⁰ The fractions eluted with 5% EtOAc in *iso*-hexane were purified by column chromatography on a Sephadex LH-20 column (CH₂Cl₂–CH₃OH; 1:1), followed by recrystallization from CH₂Cl₂–CH₃OH (1:1) to afford rhodimer (**1**, 15 mg). The fractions eluted with 6% EtOAc in *iso*-hexane were subjected to column chromatography on a Sephadex LH-20 (CH₂Cl₂–CH₃OH (1:1)) system to give quercetol B (**9**, 300 mg).¹¹ The fractions eluted with 7% EtOAc in *iso*-hexane were purified by column chromatography on a Sephadex LH-20 column (CH₂Cl₂–CH₃OH (1:1)) to give maackiain (**10**, 20 mg),¹² 6a-hydroxymaackiain (**11**, 10 mg),¹³ and pisatin (**12**, 5 mg).¹⁴ The fractions eluted with 8% EtOAc in *iso*-hexane were subjected to column chromatography on a silica gel (200 g) with 3% EtOAc in *iso*-hexane to give tephrowatsin A (**21**, 10 mg),⁸ with 5% EtOAc in *iso*-hexane to give rhodiflavan A (**2**, 50 mg), and with 10% EtOAc in *iso*-hexane to provide rhodiflavan B (**3**, 20 mg) and rhodiflavan C (**4**, 15 mg), which were further purified by preparative HPLC (CH₃OH–H₂O gradient elution). The fractions eluted with 9%–10% EtOAc in *iso*-hexane were combined and purified by column chromatography on a Sephadex LH-20 column (CH₂Cl₂–CH₃OH; 1:1), and subsequently by preparative HPLC (CH₃OH–H₂O gradient elution) to give tephrosin (**13**, 10 mg),¹⁵ rotenone (**14**, 15 mg),¹⁵ 6-hydroxyrotenone (**15**, 10 mg),¹⁶ 12a-hydroxyrotenone (**15**, 10 mg),¹⁷ rhodacarpin (**5**, 10 mg), hildecarpin (**17**, 10 mg),¹⁸ and 3-hydroxy-2-methoxy-8–9-methylenedioxypycocarpene (**18**, 15 mg).¹⁹ The fractions eluted with 12% EtOAc in *iso*-hexane gave isoliquiritigenin (**19**, 15 mg),²⁰ and those eluted with 20% EtOAc in *iso*-hexane gave D-pinitol (**20**, 900 mg).²¹

Rhodimer (1). White crystals (CH₂Cl₂–CH₃OH; 1:1); [α]_D²⁰ +13.4 (c 0.001, CH₃OH); UV (CH₂Cl₂) λ_{\max} (log ϵ) 230 (4.05), 290 (4.25), and 350 (4.30) nm; ECD (c 0.05, CH₃OH) λ_{\max} ($\Delta\epsilon$) 314 (10.16), 292 (–40.36), 249 (–23.33), 235 (50.08), 220 (–56.36), 212 (62.23); ¹H and ¹³C NMR, see Table 1; HREIMS *m/z* 660.3095 [M]⁺ (calcd for C₄₂H₄₄O₇, 660.3087).

Rhodiflavan A (2). Yellow oily paste; [α]_D²⁰ +17.5 (c 0.001, CH₂Cl₂); UV (CH₂Cl₂) λ_{\max} (log ϵ) 240 (3.05) and 290 (3.40) nm; ECD (c 0.05, CH₃OH) λ_{\max} ($\Delta\epsilon$) 300 (–92.25), 257 (85.45), 243 (–119.45); ¹H and ¹³C NMR, see Table 2; HRESIMS *m/z* 479.2493 [M + H]⁺ (calcd for C₃₀H₃₈O₅, 479.2753).

Rhodiflavan B (3). Yellow oily paste; [α]_D²⁰ +66.1 (c 0.001, CH₂Cl₂); UV (CH₂Cl₂) λ_{\max} (log ϵ) 230 (3.08) and 280 (3.20) nm; ECD (c 0.05, CH₃OH) λ_{\max} ($\Delta\epsilon$) 301 (199.73), 257 (–130.29), 225 (65.0); ¹H and ¹³C NMR, see Table 2; HRESIMS *m/z* 479.2493 [M + H]⁺ (calcd for C₃₀H₃₈O₅, 479.2753).

Rhodiflavan C (4). Yellow oily paste. [α]_D²⁰ +90.0 (c 0.001, CH₂Cl₂); UV (CH₂Cl₂) λ_{\max} (log ϵ) 230 (3.20) and 270 (3.08) nm; ECD (c 0.05, CH₃OH) λ_{\max} ($\Delta\epsilon$) 316 (89.0), 284 (–32.21), 245

(91.80), 226 (–26.26), 218 (70.0), 210 (80.5); ¹H and ¹³C NMR, see Table 3; HREIMS *m/z* 381.2062 [M]⁺ (calcd for C₂₄H₂₈O₄, 381.2066).

Rhodacarpin (5). White amorphous solid; UV (CH₂Cl₂) λ_{\max} (log ϵ) 230 (3.04), 290 (3.45), 310 (3.42) and 350 (3.10) nm; ECD (c 0.05, CH₃OH) λ_{\max} ($\Delta\epsilon$) 309 (12.0), 241 (–82.1), 220 (7.0), 205 (–80); ¹H and ¹³C NMR, see Table 4; HRESIMS *m/z* 369.1367 [M + H]⁺ (calcd for C₂₁H₂₀O₆, 369.1338).

Plasmodium falciparum Culture. In vitro parasite culture of the *P. falciparum* strain 3D7 was maintained in RPMI with 10 mM Hepes (Life Technologies), 50 μ g/mL hypoxanthine (Sigma) and 5% human serum from male AB plasma and 2.5 mg/mL AlbuMAX II (Life Technologies). Human O⁺ erythrocytes were obtained from the Australian Red Cross Blood Service (Agreement No. 13-04QLD-09; 17-06QLD-16). The parasites were maintained at 2%–8% parasitaemia (% P) at 5% hematocrit (% H), and incubated at 37 °C, 5% CO₂, 5% O₂, 90% N₂ and 95% humidity.

Plasmodium falciparum Growth Inhibition Assay. A well-established asexual *P. falciparum* imaging assay was used to determine parasite growth inhibition according to the procedure described by Duffy and Avery.³¹

Computation. A low-energy conformation library of postulated compounds **2** and **3** were generated using MacroModel as implemented in the MacroModel v12.1 Schrödinger suite by performing careful Monte Carlo conformational analysis using MMFF force fields, each with the GB/SA solvation models CHCl₃ and H₂O. Elimination of redundant conformations was performed by comparison of heavy atom coordinates applying an RMSD cutoff set to 2.0 Å. Next, all unique conformers were optimized at the B3LYP/6-311++G(3df,2pd) level of theory. The conformers having a Boltzmann weight, calculated using ΔH° , above 1% were selected for subsequent TD-DFT calculations at the same level of theory using 50 singlet excited states. To obtain the Boltzmann-weighted ECD spectrum, the individual spectra were line-broadened using a Gaussian band shape (σ = 0.3 eV). All (TD-)DFT calculations were performed using Gaussian 16, Revision A.03.³³ The solvent was taken into account by using the integral equation formalism model (IEFPCM) as implemented in Gaussian 16 and the dielectric constant for methanol (ϵ = 32.613). To compensate for the typical underestimation of the transition energies, a 20 nm blue shift was applied on the computed ECD spectra for comparison with the experimental one.³⁴

■ ASSOCIATED CONTENT

Supporting Information

CCDC 1987379 has been deposited with the Cambridge Crystallographic Data Centre. Copies of the data can be obtained, free of charge, on application to the Director, CCDC, 12 Union Road, Cambridge CB2 1EZ, U.K. (fax: +44-(0)1223-336033 or e-mail: deposit@ccdc.cam.ac.uk). The Supporting Information is available free of charge at <https://pubs.acs.org/doi/10.1021/acs.jnatprod.0c00245>.

Original MS and NMR spectra for all compounds, along with the corresponding NMReDATA³⁵ for the new compounds **1–5**; the X-ray structure of **1** (details are freely available on Zenodo at <https://10.5281/zenodo.3679345>); NMR and MS data for compounds (**1–21**) (PDF)

Crystallographic data for **1** (CIF)

■ AUTHOR INFORMATION

Corresponding Authors

Máté Erdélyi – Department of Chemistry—BMC, Uppsala University, SE-751 23 Uppsala, Sweden; Department of Chemistry and Molecular Biology, University of Gothenburg, SE-412 96 Gothenburg, Sweden; orcid.org/0000-0003-

0359-5970; Phone: +46-72-9999166; Email: mate.erdelyi@kemi.uu.se

Abiy Yenesew – Department of Chemistry, University of Nairobi, 30197-00100 Nairobi, Kenya; Phone: +254 733 832 576; Email: ayenesew@uonbi.ac.ke

Authors

Yoseph Atilaw – Department of Chemistry, University of Nairobi, 30197-00100 Nairobi, Kenya; Department of Chemistry—BMC, Uppsala University, SE-751 23 Uppsala, Sweden

Lois Muiva-Mutisya – Department of Chemistry, University of Nairobi, 30197-00100 Nairobi, Kenya

Jonathan Bogaerts – Department of Chemistry, University of Antwerp, B-2020 Antwerp, Belgium

Sandra Duffy – Discovery Biology, Griffith Institute for Drug Discovery, Griffith University, Nathan, Qld 4111, Australia

Arto Valkonen – University of Jyväskylä, Department of Chemistry, FI-40014 Jyväskylä, Finland; orcid.org/0000-0003-2806-3807

Matthias Heydenreich – Institut für Chemie, Universität Potsdam, D-14476 Potsdam, Germany

Vicky M. Avery – Discovery Biology, Griffith Institute for Drug Discovery, Griffith University, Nathan, Qld 4111, Australia

Kari Rissanen – University of Jyväskylä, Department of Chemistry, FI-40014 Jyväskylä, Finland; orcid.org/0000-0002-7282-8419

Complete contact information is available at:

<https://pubs.acs.org/10.1021/acs.jnatprod.0c00245>

Notes

The authors declare no competing financial interest.

ACKNOWLEDGMENTS

Y.A. is grateful to the German Academic Exchange Services (DAAD) for a scholarship that was offered through the Natural Products Research Network for Eastern and Central Africa (NAPRECA). The Swedish Research Council (Swedish Research Links, NOs. 2012-6124 and 2019-03715), the International Science Program (ISP Sweden, Grant No. KEN-02), and the Australian Research Council (Grant No. LP120200557 to V.M.A.) are gratefully acknowledged for financial support. We thank the Australian Red Cross Blood Service for the provision of human blood. Jonathan Bogaerts thanks the Research foundation Flanders (FWO-Vlaanderen) for the appointment of a predoctoral scholarship (No. 1198318N) and acknowledges the Flemish Supercomputing Centre (VSC) for providing computational resources and support. The Academy of Finland (Grant No. 314343 to A.V.) is also gratefully acknowledged for funding. The Swedish NMR Centre is acknowledged for access to an 800 MHz spectrometer.

REFERENCES

- (1) Chen, Y.; Yan, T.; Gao, C.; Cao, W.; Huang, R. *Molecules* **2014**, *19*, 1432–1458.
- (2) Muiva, L. M.; Yenesew, A.; Derese, S.; Heydenreich, M.; Peter, M. G.; Akala, H. M.; Eyase, F.; Waters, N. C.; Mutai, C.; Keriko, J. M.; Walsh, D. *Phytochem. Lett.* **2009**, *2*, 99–102.
- (3) Juma, W. P.; Akala, H. M.; Eyase, F. L.; Muiva, L. M.; Heydenreich, M.; Okalebo, F. A.; Gitu, P. M.; Peter, M. G.; Walsh, D. S.; Imbuga, M.; Yenesew, A. *Phytochem. Lett.* **2011**, *4*, 176–178.

- (4) Touqeer, S.; Saeed, M. A.; Ajaib, M. *Phytopharmacology* **2013**, *4*, 598–637.
- (5) Muiva-Mutisya, L.; Macharia, B.; Heydenreich, M.; Koch, A.; Akala, H. M.; Derese, S.; Omosa, L. K.; Yusuf, A. O.; Kamau, E.; Yenesew, A. *Phytochem. Lett.* **2014**, *10*, 179–183.
- (6) Atilaw, Y.; Muiva-Mutisya, L.; Ndakala, A.; Akala, H. M.; Yeda, R.; Wu, Y. J.; Coghi, P.; Wong, V. K. W.; Erdélyi, M.; Yenesew, A. *Molecules* **2017**, *22*, 1514.
- (7) Atilaw, Y.; Duffy, S.; Heydenreich, M.; Muiva-Mutisya, L.; Avery, V. M.; Erdélyi, M.; Yenesew, A. *Molecules* **2017**, *22*, 318.
- (8) Gomez, F.; Quijano, L.; Calderon, J. S.; Rodriguez, C.; Rios, T. *Phytochemistry* **1985**, *24*, 1057–1059.
- (9) Dagne, E.; Mammo, W.; Sterner, O. *Phytochemistry* **1992**, *31*, 3662–3663.
- (10) Céspedes, C. L.; Achnine, L.; Lotina-Hennsen, B.; Salazar, J. R.; Gómez-Garibay, F.; Calderón, J. S. *Pestic. Biochem. Physiol.* **2001**, *69*, 63–76.
- (11) Gomez-Garibay, F.; Quijano, L.; Calderon, J. S.; Morales, S.; Rios, T. *Phytochemistry* **1988**, *27*, 2971–2973.
- (12) Mizuno, M.; Tanaka, T.; Katsuragawa, M.; Saito, H.; Iinuma, M. *J. Nat. Prod.* **1990**, *53*, 498–499.
- (13) Bilton, J. N.; Debnam, J. R.; Smith, I. M. *Phytochemistry* **1976**, *15*, 1411–1412.
- (14) Kobayashi, A.; Akiyama, K.; Kawazu, K. *Phytochemistry* **1992**, *32*, 77–78.
- (15) Stevenson, P. C.; Kite, G. C.; Lewis, G. P.; Forest, F.; Nyirenda, S. P.; Belmain, S. R.; Sileshi, G. W.; Veitch, N. C. *Phytochemistry* **2012**, *78*, 135–146.
- (16) Krupadanam, G. L. D.; Srimannarayana, G.; Rao, N. V. S. *Indian J. Chem., Sect. B* **1978**, *16B*, 770–772.
- (17) Oberholzer, M. E.; Rall, G. J. H.; Roux, D. G. *Phytochemistry* **1976**, *15*, 1283–1284.
- (18) Lwande, W.; Bentley, M. D.; Macfoy, C.; Lugemwa, F. N.; Hassanali, A.; Nyandat, E. *Phytochemistry* **1987**, *26*, 2425–2426.
- (19) Lwande, W.; Bentley, M. D.; Hassanali, A. *Int. J. Trop. Insect Sci.* **1986**, *7*, 501–503.
- (20) Takahashi, T.; Takasuka, N.; Iigo, M.; Baba, M.; Nishino, H.; Tsuda, H.; Okuyama, T. *Cancer Sci.* **2004**, *95*, 448–453.
- (21) Raya-Gonzalez, D.; Pamatz-Bolanos, T.; del Rio-Torres, Rosa E. d.; Martinez-Munoz, R. E.; Ron-Echeverria, O.; Martinez-Pacheco, M. M. Z. *Naturforsch., C: J. Biosci.* **2008**, *63*, 922–924.
- (22) Yan, X.-T.; Li, W.; Sun, Y.-N.; Yang, S.-Y.; Lee, S.-H.; Chen, J.-B.; Jang, H.-D.; Kim, Y.-H. *Bioorg. Med. Chem. Lett.* **2014**, *24*, 1397–1402.
- (23) Asada, Y.; Sukemori, A.; Watanabe, T.; Malla, K. J.; Yoshikawa, T.; Li, W.; Kuang, X.; Koike, K.; Chen, C.-H.; Akiyama, T.; Qian, K.; Nakagawa-Goto, K.; Morris-Natschke, S. L.; Lu, Y.; Lee, K.-H. *J. Nat. Prod.* **2013**, *76*, 852–857.
- (24) Bogorad, L. *Annu. Rev. Plant Physiol.* **1958**, *9*, 417–448.
- (25) Slade, D.; Ferreira, D.; Marais, J. P. J. *Phytochemistry* **2005**, *66*, 2177–2215.
- (26) Pouget, C.; Fagnere, C.; Basly, J.-P.; Leveque, H.; Chulia, A.-J. *Tetrahedron* **2000**, *56*, 6047–6052.
- (27) Mai, H. D.; Nguyen, T. T.; Pham, V. C.; Litaudon, M.; Gueritte, F.; Tran, D. T.; Nguyen, V. H. *Planta Med.* **2010**, *76*, 1739–1742.
- (28) Soby, S.; Bates, R.; van Etten, H. *Phytochemistry* **1997**, *45*, 925–929.
- (29) Soby, S.; Caldera, S.; Bates, R.; VanEtten, H. *Phytochemistry* **1996**, *41*, 759–765.
- (30) Goel, A.; Kumar, A.; Raghuvanshi, A. *Chem. Rev.* **2013**, *113*, 1614–1640.
- (31) Duffy, S.; Avery, V. M. *Am. J. Trop. Med. Hyg.* **2012**, *86*, 84–92.
- (32) Mishra, L. C.; Bhattacharya, A.; Bhasin, V. K. *Acta Trop.* **2009**, *109*, 194–198.
- (33) Frisch, M. J.; Trucks, G. W.; Schlegel, H. B.; Scuseria, G. E.; Robb, M. A.; Cheeseman, J. R.; Scalmani, G.; Barone, V.; Petersson, G. A.; Nakatsuji, H.; Li, X.; Caricato, M.; Marenich, A. V.; Bloino, J.; Janesko, B. G.; Gomperts, R.; Mennucci, B.; Hratchian, H. P.; Ortiz, J.

V.; Izmaylov, A. F.; Sonnenberg, J. L.; Williams Ding, F.; Lipparini, F.; Egidi, F.; Goings, J.; Peng, B.; Petrone, A.; Henderson, T.; Ranasinghe, D.; Zakrzewski, V. G.; Gao, J.; Rega, N.; Zheng, G.; Liang, W.; Hada, M.; Ehara, M.; Toyota, K.; Fukuda, R.; Hasegawa, J.; Ishida, M.; Nakajima, T.; Honda, Y.; Kitao, O.; Nakai, H.; Vreven, T.; Throssell, K.; Montgomery, J. A., Jr.; Peralta, J. E.; Ogliaro, F.; Bearpark, M. J.; Heyd, J. J.; Brothers, E. N.; Kudin, K. N.; Staroverov, V. N.; Keith, T. A.; Kobayashi, R.; Normand, J.; Raghavachari, K.; Rendell, A. P.; Burant, J. C.; Iyengar, S. S.; Tomasi, J.; Cossi, M.; Millam, J. M.; Klene, M.; Adamo, C.; Cammi, R.; Ochterski, J. W.; Martin, R. L.; Morokuma, K.; Farkas, O.; Foresman, J. B.; Fox, D. J. *Gaussian 16, Revision C.01*; Gaussian: Wallingford, CT, 2016.

(34) Autschbach, J. Ab Initio Electronic Circular Dichroism and Optical Rotatory Dispersion: from Organic Molecules to Transition Metal Complexes. In *Comprehensive Chiroptical Spectroscopy: Instrumentation, Methodologies, and Theoretical Simulations*, Vol. 1; John Wiley & Sons, 2012; Chapter 21, pp 593–642.

(35) Pupier, M.; Nuzillard, J. M.; Wist, J.; Schlörer, N. E.; Kuhn, S.; Erdelyi, M.; Steinbeck, C.; Williams, A. J.; Butts, C.; Claridge, T. D. W.; Mikhova, B.; Robien, W.; Dashti, H.; Eghbalnia, H. R.; Fares, C.; Adam, C.; Kessler, P.; Moriaud, F.; Elyashberg, M.; Argyropoulos, D.; Perez, M.; Giraudeau, P.; Gil, R. R.; Trevorow, P.; Jeannerat, D. *Magn. Reson. Chem.* **2018**, *56*, 703–715.